# Photophysical and Theoretical Studies on the Stereoselective Complexation of Naphthylethanols with β-Cyclodextrin†

R. S. Murphy,‡ T. C. Barros,‡ B. Mayer,*,§ G. Marconi,*,|| and C. Bohne*,‡

*Department of Chemistry, University of Victoria, P.O. Box 3065, Victoria, BC, Canada V8W 3V6, Institute for Theoretical Chemistry and Molecular Structural Biology, University of Vienna, UZAII, Althanstrasse 14, A-1090 Vienna, Austria, and Istituto FRAE-CNR, via Gobetti 101, 40129 Bologna, Italy*

*Received April 10, 2000. In Final Form: July 4, 2000*

Stereoselective binding of the 1-naphthyl-1-ethanol (1-NpOH) and 2-naphthyl-1-ethanol (2-NpOH) enantiomers with β-cyclodextrin (β-CD) was investigated by photophysical and theoretical studies. The latter are based on structural calculations of the complexes and their respective induced circular dichroism spectra. For the enantiomers of 1-NpOH, where the complexes with β-CD have a 1:1 (guest:CD) stoichiometry, a mixture of structures with different geometries was observed for each enantiomer. No stereoselectivity was apparent for these complexes. (*R*)- and (*S*)-2-NpOH form complexes with β-CD that have both 1:1 and 2:2 stoichiometries. Structural calculations indicate that the naphthyl moiety of both enantiomers is preferentially included in the CD cavity for the 1:1 complex. In the case of the complexes with 2:2 stoichiometry, a mixture of complexes is present that either have the naphthyl moieties at a distance or in close proximity. The former geometry explains the observation of long-lived excited triplet states for 2-NpOH, whereas the latter geometry is responsible for the excimer emission. The stereoselectivity observed for the monomer to excimer intensity ratios when (*R*)- and (*S*)-2-NpOH are complexed to β-CD is due to the different contributions of 2:2 complexes with different geometries.

## Introduction

Cyclodextrins (CDs) are cyclic molecules made of D-glucose units. The internal cavity of CDs is relatively hydrophobic and lends itself for inclusion of guest molecules. CDs are versatile hosts because the size of their cavities can be regulated by the number of glucose units (6, 7, or 8 for α-, β-, and γ-CD) in each molecule, and the alcohol groups at the rims of the cavities can be functionalized.[1−6] For this reason, CDs have been employed to study a variety of fundamental issues in supramolecular chemistry and for industrial applications where they are used in chiral separation technology and drug delivery.[6,7]

CDs form complexes with a variety of inorganic and organic compounds. The thermodynamics of complexation has been extensively studied, and a wealth of information is available on how the guest's structure influences the efficiency of complex formation.[8,9] CDs can form complexes with different inclusion modes. For example, the guest can be deeply included in the CD cavity or can interact only with the rim of the cavity.[10] NMR spectroscopy and induced circular dichroism spectra (ICD) have been employed to study the inclusion of guests in CDs.[11−27] In the case of NMR, the shift of signals corresponding to the CD hydrogens located inside the cavity indicates that the

† Part of the special issue "Colloid Science Matured, Four Colloid Scientists Turn 60 at the Millennium". This paper is dedicated to Professors Amlgren, Holzwarth, Mackay, and Wyn-Jones on the occasion of their 60th birthdays.

* Corresponding author. Phone: 250-721-7151. Fax: 250-721-7147. E-mail: bohne@uvic.ca; http://foto.chem.uvic.ca/

‡ University of Victoria.

§ University of Vienna. E-mail: bernd.mayer@univie.ac.at; http://asterix.msp.univie.ac.at/local-link.

|| Instituto FRAE-CNR. E-mail: marc@frae.bo.cnr.it; http://frae.bo.cnr.it/marc.

(1) Saenger, W. *Angew. Chem., Int. Ed. Engl.* **1980**, *19*, 344.
(2) Tabushi, I. *Acc. Chem. Res.* **1982**, *15*, 66.
(3) Szejtli, J. Chemistry, Physical and Biological Properties of Cyclodextrins. In *Cyclodextrins*; Szejtli, J., Osa, T., Eds.; Elsevier Science Ltd.: New York, 1996; Vol. 3, p 5.
(4) Szejtli, J. *Cyclodextrin Technology*, 1st ed.; Kluwer Academic Publishers: Dordrecht, The Netherlands, 1988.
(5) Jicsinszky, L.; Fenyvesi, E.; Hashimoto, H.; Ueno, A. Cyclodextrin Derivatives. In *Cyclodextrins*; Szejtli, J., Osa, T., Eds.; Elsevier Science Ltd.: New York, 1996; Vol. 3, p 57.
(6) Li, S.; Purdy, W. C. *Chem. Rev.* **1992**, *92*, 1457.
(7) Uekama, K.; Hirayama, F.; Irie, T. *Chem. Rev.* **1998**, *98*, 2045.
(8) Connors, K. A. *J. Pharm. Sci.* **1995**, *84*, 843.
(9) Connors, K. A. Measurement of Cyclodextrin Complex Stability Constants. In *Cyclodextrins*; Szejtli, J., Osa, T., Eds.; Elsevier Science Ltd.: New York, 1996; Vol. 3, p 205.
(10) Linert, W.; Margl, P.; Lukowitz, I. *J. Comput. Chem.* **1992**, *16*, 61.
(11) Demarco, P. V.; Thakkar, A. L. *Chem. Commun.* **1970**, 2.
(12) Lipkowitz, K. B.; Raghothama, S.; Yang, J. *J. Am. Chem. Soc.* **1992**, *114*, 1554.
(13) Muñoz de la Peña, A.; Ndou, T. T.; Zung, J. B.; Greene, K. L.; Live, D. H.; Warner, I. M. *J. Am. Chem. Soc.* **1991**, *113*, 1572.
(14) McAlpine, S. R.; Garcia-Garibay, M. A. *J. Org. Chem.* **1996**, *61*, 8307.
(15) Schneider, H.-J.; Blater, T.; Simova, S. *J. Am. Chem. Soc.* **1991**, *113*, 1996.
(16) Harata, K.; Uedaira, H. *Bull. Chem. Soc. Jpn.* **1975**, *48*, 375.
(17) Kamiya, M.; Mitsuhashi, S.; Makino, M.; Yoshioka, H. *J. Phys. Chem.* **1992**, *96*, 95.
(18) Kodaka, M. *J. Phys. Chem.* **1991**, *95*, 2110.
(19) Kodaka, M. *J. Am. Chem. Soc.* **1993**, *115*, 3702.
(20) Marconi, G.; Monti, S.; Mayer, B.; Köhler, G. *J. Phys. Chem.* **1995**, *99*, 3943.
(21) Marconi, G.; Mayer, B. *Pure Appl. Chem.* **1997**, *69*, 779.
(22) Grabner, G.; Monti, S.; Marconi, G.; Mayer, B.; Klein, C. T.; Köhler, G. *J. Phys. Chem.* **1996**, *100*, 20068.
(23) Mayer, B.; Klein, C. T.; Marconi, G.; Köhler, G. *J. Incl. Phenom. Mol. Recognit. Chem.* **1997**, *29*, 79.
(24) Schneider, H.-J.; Hacket, F.; Rüdiger, V. *Chem. Rev.* **1998**, *98*, 1755.
(25) Murphy, R. S.; Barros, T. C.; Barnes, J.; Mayer, B.; Marconi, G.; Bohne, C. *J. Phys. Chem. A* **1999**, *103*, 137.
(26) Zhang, X.; Nau, W. R. *Angew. Chem., Int. Ed. Engl.* 2000, *39*, 544.
(27) Grabner, G.; Rechthalter, K.; Mayer, B.; Köhler, G. *J. Phys. Chem. A* 2000, *104*, 1365.

10.1021/la0005311 CCC: $19.00 
Published on Web 09/30/2000

**Chart 1**

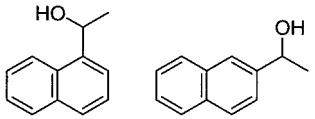


1-NpOH 2-NpOH

guest is incorporated within the cavity. ICD spectra are observed for achiral guests when these molecules interact with the chiral CD cavity. In the case of chiral molecules, the guest shows a circular dichroism signal in water and the ICD signals due to the complexation of the guest appear as signal enhancements or changes in the signal's sign. In general, the sign and strength of the ICD signal are related to the distance and orientation of the transition dipole moment of the guest with respect to the nonsymmetric bonds of the CD framework. In a simplified geometrical theory, CD was assumed to be a truncated cone. When the guest is deeply incorporated into the CD cavity, the sign of the ICD signal was assigned to parallel (+) or perpendicular (−) alignment of the guest's transition moment with that of the CD cavity. The opposite rule should hold for an external attachment of the guest to the host.[17−19] However, this simple model is applicable only to extreme situations, because the real nature of the host−guest complexation is only reproducible by calculations in which a sequence of intermediate and highly variable reciprocal positions between host and guest are considered. Recently, computational chemistry has been applied to gain structural information on CD complexes.[28] Previous work established that one approach is to combine statistical optimizations of the host−guest structures obtained from dynamic Monte Carlo calculations with a modified version of the Kirkwood−Tinoco framework for the calculations of ICD spectra.[22,23,29] It is worth noting that solvation effects and hydrophobic interactions are important prerequisites for obtaining the correct CD complex geometries.[23] The calculated ICD spectra for the CD host−guest structures with low energies are compared to experimental ICD spectra to validate the calculations.

Detailed knowledge of the structure of CD−guest complexes is important for understanding the thermodynamic stability of the complex and the guest's complexation dynamics. Recently, we have made a concerted effort to understand the parameters that influence the entry/exit rate constants of guests with CDs. Most studies centered on xanthone,[30−32] because its unique photophysics [33−35] makes it possible to directly follow the relocation of the triplet excited state from the CD cavity into water. Theoretical calculations combined with experimental ICD spectra showed that xanthone interacts with the rim of the CD cavity containing the secondary alcohol groups and does not penetrate deeply into the CD cavity.[25] When the enantiomers of 1-naphthyl-1-ethanol (1-NpOH) and 2-naphthyl-1-ethanol (2-NpOH) (Chart 1) were used as guest molecules with β-CD, a much slower exit rate constant from the 1:1 (guest:CD) complex was measured ($(2-5) \times 10^5$ $s^{-1}$)[36] than that observed for xanthone ($8.4 \times 10^6$ $s^{-1}$).[31] In addition, in the case of 2-NpOH a 2:2 complex (higher order complex) was formed which led to the observation of excimer emission. The dissociation of 2-NpOH from the 2:2 complex was estimated to be at least 2 orders of magnitude slower ($10^3$ $s^{-1}$) than the exit from the 1:1 complex.[36] Both NpOHs are chiral, and we explore in this work if stereoselective binding motifs for the 1:1 complexes of the enantiomers of 1-NpOH and 2-NpOH with β-CD and the 2:2 complex of 2-NpOH could be uncovered from theoretical calculations and experimental photophysical studies. Our results show that no unambiguous complex was formed for the enantiomers of NpOH with β-CD, suggesting that a mixture of complexes with different structures was observed. This result has consequences for the interpretation of the dynamics of host−guest complexes where the guest is asymmetrical and also explains why excimer emission and long-lived excited triplet states can be observed in this system.

## Experimental Section

**Experimental Methods.** (*R*)- and (*S*)-1-NpOH, and (*R*)- and (*S*)-2-NpOH (Fluka) were used as received. The β−CD sample (lots C6 034−13 or F6080−191) was a generous gift from Cerestar and was used without further purification. All samples were prepared with deionized water (Sybron-Barnstead). NpOH solutions of each enantiomer (50, 150, or 300 μM) were prepared by injecting a small amount of a methanolic stock solution (10 mM) into water. The stock solutions containing CDs (10 and 1 mM) were prepared by dissolving the solid in the aqueous NpOH solutions. Different CD concentrations were achieved by diluting the CD stock solutions with the aqueous NpOH solution. All CD solutions were stirred for at least 12 h.

UV−vis absorption spectra were recorded on a Cary 1 or a Cary 5 spectrometer. Steady-state fluorescence spectra were measured with a PTI QM-2 spectrofluorimeter at 20.0 ± 0.5 °C. The excitation wavelengths were 280 or 305 nm, and the excitation and emission slits were set to obtain a band-pass between 2 and 3 nm. A PTI LS-1 single photon counter was employed to measure the fluorescence decay (20.0 ± 0.5 °C) where mostly the monomer ($\lambda_{ex} = 280$ nm, $\lambda_{em} = 360$ nm) and mostly the excimer ($\lambda_{ex} = 280$ nm, $\lambda_{em} = 405$ nm) emit. The instrument response function was collected with suspended silica gel in water. Visual analysis of the residuals, the autocorrelation function, and evaluation of $\chi^2$ values were used to establish the goodness of the fit to the experimental data.

The laser flash photolysis system used to obtain the triplet−triplet absorption spectra has been previously described.[32] Samples were excited at 266 nm with a Spectra-Physics YAG (GCR-12) laser. NpOHs in aqueous solutions are easily photoionized.[36] A flow cell (7 mm × 7 mm, Suprasil) was employed to ensure that for each laser shot a fresh solution was irradiated. The reservoir containing the solution used for the flow setup was purged with $N_2$ for at least 30 min.

Circular dichroism spectra were recorded with a Jasco-810 spectropolarimeter. The scan rate, bandwidth, and integration times were 20 nm/min, 1 nm, and 8 s, respectively. The system was extensively purged with $N_2$ before spectra were acquired. Cylindrical quartz cells with either 1 mm or 10 mm path lengths were used, and all measurements were recorded at room temperature (20 ± 2 °C). A baseline was collected before each experiment by using an empty cell. When the signal of an achiral molecule (naphthalene) in water was measured, it was observed that the signal-to-noise ratio was very poor when the photomultiplier voltage was higher than 300 V. For this reason, the spectra for NpOH and NpOH/CD above 230 nm were collected in a cell with a path length of 10 mm, whereas a second spectrum below 230 nm was collected with a 1 mm path length cell. The spectra were imported into the Kaleidagraph program, the path lengths were normalized, and both spectra were combined. All spectra were normalized to unity at the maximum ellipticity observed.

(28) Lipkowitz, K. B. *Chem. Rev.* **1998**, *98*, 1829.
(29) Mayer, B.; Klein, C. T.; Topchieva, I.; Köhler, G. *J. Comput.-Aided Mol. Des.* **1999**, *13*, 373.
(30) Barra, M.; Bohne, C.; Scaiano, J. C. *J. Am. Chem. Soc.* **1990**, *112*, 8075.
(31) Liao, Y.; Frank, J.; Holzwarth, J. F.; Bohne, C. *J. Chem. Soc., Chem. Commun.* **1995**, 199.
(32) Liao, Y.; Bohne, C. *J. Phys. Chem.* **1996**, *100*, 734.
(33) Scaiano, J. C. *J. Am. Chem. Soc.* **1980**, *102*, 7747.
(34) Abuin, E. B.; Scaiano, J. C. *J. Am. Chem. Soc.* **1984**, *106*, 6274.
(35) Evans, C. H.; Prud'homme, N.; King, M.; Scaiano, J. C. *J. Photochem. Photobiol. A: Chem.* **1999**, *121*, 105.
(36) Barros, T. C.; Stefaniak, K.; Holzwarth, J. F.; Bohne, C. *J. Phys. Chem. A* **1998**, *102*, 5639.

**Theoretical Methods.** *Calculation of Low-Energy Structures for the CD Complexes.* The computation of the potential energies for the 1:1 and 2:2 complexes between NpOHs and $\beta$-CD was based on Allinger's MM3-92 force field by applying a block diagonal matrix minimization method.[37] The fully minimized reference structure of $\beta$-CD, derived from crystallographic data,[38] gave an energy of 71.3 kcal/mol. The potential energy of the (*R*)-1-NpOH and (*S*)-1-NpOH were calculated to be 6.76 and 8.13 kcal/mol, respectively. The values for 2-NpOH were determined to be 4.58 kcal/mol for the *R*- and 5.55 kcal/mol for the *S*-enantiomers. These reference structures were used in all calculations described below.

Low-energy complex geometries were located by applying a Dynamic Monte Carlo (DMC) routine[39,40] within the program package MultiMize.[41] The potential energies were calculated using the force field. The solvation effects were calculated by a continuum approximation using the Wesson−Eisenberg solvation parameters,[42] and the solvation energies were −50.03 kcal/mol for $\beta$-CD, 0.97 and 1.03 kcal/mol for (*R*)- and (*S*)-1-NpOH and 0.63 and 0.70 kcal/mol for (*R*)- and (*S*)-2-NpOH. Both, the potential energies and solvation effects were considered in a modified Metropolis criterion.[23] The start geometries for DMC runs were defined by a random relative orientation of host and guest molecule(s) within a distance of 5 Å. In the case of the NpOHs two principal relative arrangements were defined as DMC start structures: (i) the naphthyl group faced the secondary hydroxyl rim of the CD ((*na*) configuration) and (ii) the ethanol group faced the secondary hydroxyl rim of the macrocycle ((*et)* configuration). In each DMC step, the host and guest positions were stochastically altered in the *x*, *y*, and *z* axes by a maximum of 0.5 Å, whereas the guests and the individual glucose units of the CDs were rotated by a maximum of 5°. Each stochastically generated structure was fully minimized within the force field and accepted according to the modified Metropolis criterion.[41] The simulation temperature was kept constant at 300 K and low-energy complex structures were obtained within 1000 DMC steps for 1:1 and 2500 DMC steps for 2:2 complexes. Fully minimized *(na)* geometries were characterized by having the naphthyl group inside the CD cavity, whereas in the *(et)* case the ethanol group was encapsulated. The total complexation energy ($E_C$) is given by the sum of the change in potential energy ($\Delta E_P$) and change in the solvation free energy ($\Delta E_S$). The value for $\Delta E_P$ corresponds to the difference between the potential energy of the complex $E_P$ and the sum of the potential energies of the isolated host and guest molecules. Likewise, the solvation energy is given by the difference in solvation energy of the complex compared to the solvation energies of the isolated compounds.

*Calculation of the Induced Circular Dichroism Spectra.* The reliability of the geometries found in the DMC calculations was tested by comparing calculated and experimental ICD spectra. In the case of 1:1 complexes, the rotational strength arises from the interaction of the dipole transition moments of the guest excited states with those at high energy (low wavelength) of the CD. The pertinent expressions were obtained by replacing the original dipole−dipole interaction scheme [43] in the Kirkwood equations by the polarizability of the bonds of the chiral macrocycle. According to this approximation, the equations of the rotatory strength for a transition $0 \rightarrow a$ are given by

$$R_{0a} = \pi \nu_a \mu_{0a}^2 \sum_j \frac{\nu_{0j}^2(\alpha_{33} - \alpha_{11})_j (GF)_j}{c(\nu_{0j}^2 - \nu_a^2)} \qquad (1)$$

$$(GF)_j = \frac{1}{r_j^3}\left[\mathbf{e}_{0a}\mathbf{e}_j - \frac{3(\mathbf{e}_{0a}\,\mathbf{r}_j)(\mathbf{e}_j\,\mathbf{r}_j)}{r_j^2}\right]\mathbf{e}_{0a} \times \mathbf{e}_j\mathbf{r}_j \qquad (2)$$

where $\mathbf{e}_{0a}$ and $\mathbf{e}_j$ are unit vectors along the electric transition moment $\mu_{0a}$ and parallel to the *j*th bond, respectively; $\nu_{0j}$ and $\nu_a$ are frequencies of the electric transitions of host and guest that are located at a distance $r_j$, and $\alpha_{11}$ and $\alpha_{33}$ represent bond polarizabilities at zero frequency, parallel and perpendicular to the symmetry axis of the bond *j*.

In the case of 2:2 complexes, an explicit interaction between the electric dipole transition moments of the two NpOHs had to be considered. Therefore, a term derived from the dimer model (Moffit exciton coupling) was added to the right-hand side of eq 1:[44]

$$R_{0a}{}^d = \pm(\pi/2\lambda)R_{12}\langle\varphi_{20}|\mu_2|\varphi_{2a}\rangle \times \langle\varphi_{10}|\mu_1|\varphi_{1a}\rangle \qquad (3)$$

This term was responsible for a characteristic sigmoidal shape of the spectrum with the zero point corresponding to the maximum of the absorption band. This term can be the dominant one (depending on the concentration of the 2:2 complex) in the ICD spectrum and can provide an immediate diagnosis of the presence of higher order complexes. Finally, for weakly allowed transitions it was important to add a term arising from the interaction of a magnetic dipole term of one of the states with the electric dipole moments of the other states.[43,44]

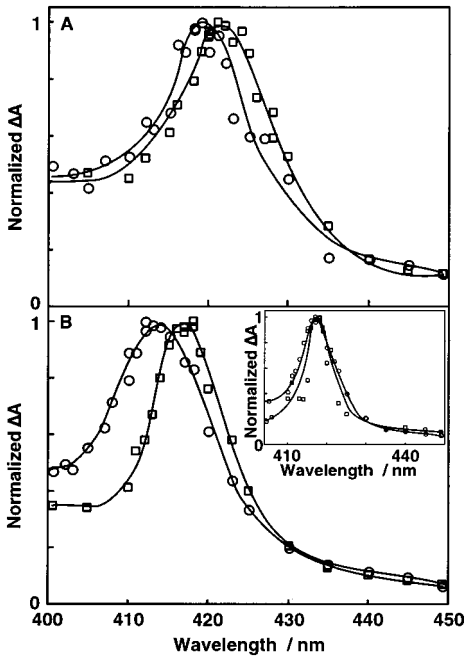


**Figure 1.** Normalized transient absorption spectra for 150 $\mu$M (*R*)-1-NpOH (A) and 150 $\mu$M (*R*)-2-NpOH (B) in the absence (○) and presence (□) of 10 mM $\beta$-CD. The inset shows the normalized transient absorption spectra of 50 (□) and 150 $\mu$M (○) (*R*)-2-NpOH in the presence of 10 mM $\beta$-CD. The solid lines were included to show the trend in the absorbance changes.

## Results and Discussion

**Complexation of 1-NpOH with $\beta$-CD.** The enantiomers of 1-NpOH were previously shown to form 1:1 complexes with $\beta$-CD (160 $M^{-1}$). There was no evidence from fluorescence or NMR binding studies for the formation of higher order complexes, i.e., complexes involving more than one CD molecule.[36]

The triplet−triplet absorption spectrum of 1-NpOH in water displayed a maximum at 420 nm. In the presence of 10 mM $\beta$-CD, 62% of the 1-NpOH molecules were complexed, and the triplet absorption maximum shifted to the red by 3 nm. The full-width at half-maximum (fwhm)

(37) Allinger, N. L.; Yuh, Y. H.; Lee, J. H. *J. Am. Chem. Soc.* **1989**, *111*, 8551.
(38) Betzel, C.; Saeger, W.; Hingerty, B. E.; Brown, G. M. *J. Am. Chem. Soc.* **1984**, *106*, 7545.
(39) Metropolis, N.; Rosenbluth, A. W.; Rosenbluth, M. B.; Teller, A. H. *J. Chem. Phys.* **1953**, *21*, 1087.
(40) Kirkpatrick, S.; Gelatt, C. D.; Vecchi, M. P. *Science* **1983**, *220*, 671.
(41) Mayer, B. *Program Package MultiMize;* University of Vienna: Vienna, Austria, 1997.
(42) Wesson, L.; Eisenberg, D. *Protein Sci.* **1992**, *1*, 227.
(43) Tinoco, I., Jr. *Adv. Chem. Phys.* **1962**, *4*, 113.
(44) Schellman, J. A. *Acc. Chem. Res.* **1968**, *1*, 144.

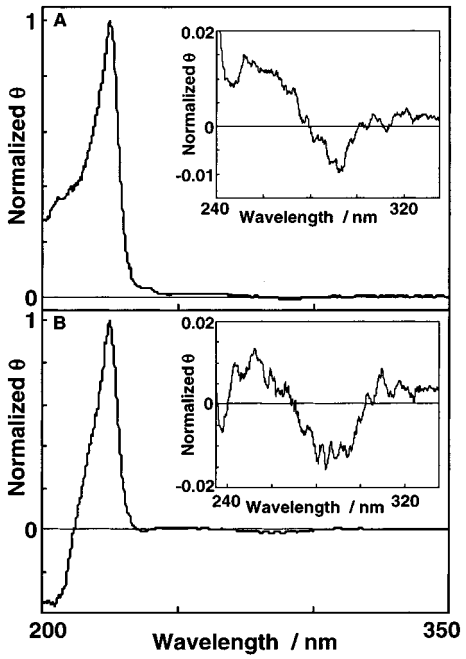


**Figure 2.** Combined and normalized ICD spectra for 150 μM (*R*)-1-NpOH (A) and 150 μM (*S*)-1-NpOH (B) in the presence of 10 mM β-CD. The normalization to unity corresponds to 7.5 and 5.2 mdeg ($l$ = 1 mm) in A and B, respectively. The insets show an expansion of the ICD spectra.

of the triplet absorption did not change (ca. 20 nm) in the presence of β-CD (Figure 1). The triplet lifetimes were long (>20 μs) in the absence and presence of CD and were limited by the presence of residual amounts of oxygen in solution. When naphthalene was included in CDs[27] or bile salt aggregates,[45] a red shift and narrowing of the triplet−triplet absorption were observed, suggesting that naphthalene was included in a structured environment and was relatively protected from water. The fact that no narrowing of the triplet−triplet absorption was observed for the 1-NpOH/β-CD complex indicates that the naphthyl chromophore was somewhat exposed to water.

In the presence of 10 mM β-CD, both enantiomers of 1-NpOH showed strong ICD signals (Figure 2). In the absence of CD, (*R*)-1-NpOH and (*S*)-1-NpOH showed weak circular dichroism signals between 200 and 240 nm that had opposite signs. Correction of the ICD spectra in the presence of β-CD for the 38% NpOH free in aqueous solution led to small decreases of the absolute intensities between 200 and 240 nm, but the features of the spectra did not change.

The calculated structures for the complexes of (*R*)-1-NpOH and (*S*)-1-NpOH showed low-energy geometries in a fairly comparable energy range (Table 1). Formation of the complex was favored by the change in potential energy, whereas the solvation effect had in most cases the opposite effect. In the case of the (*na*) geometry for (*R*)-1-NpOH, the naphthyl ring was mainly located at the rim of the CD containing the secondary alcohols. For the (*et*) geometry, the ethyl group was deeply included in the β-CD cavity, and the relative orientation of the naphthyl ring with respect to the CD axis was tilted by 90° (Figure 3). The (*et*) geometry was energetically favored by ca. 5 kcal/mol. This stabilization was a consequence of lower potential and solvation energies. The converse was observed for (*S*)-1-NpOH, where the (*na*) geometry was calculated to be more stable than the (*et*) geometry. The naphthyl group

(45) Ju, C.; Bohne, C. *J. Phys. Chem.* **1996**, *100*, 3847.

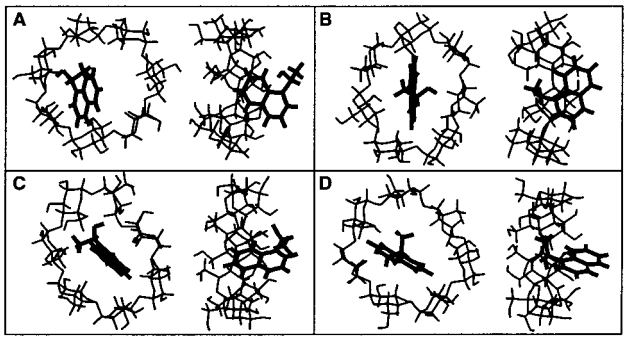


**Figure 3.** Low-energy structures calculated for the complexes between β-CD and (*R*)-1-NpOH (A, (*na*) geometry; B, (*et*) geometry) and (*S*)-1-NpOH (C, (*na*) geometry; D, (*et*) geometry).

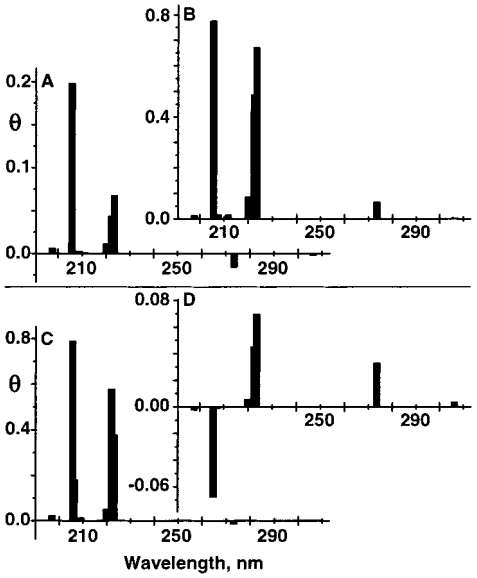


**Figure 4.** Calculated ICD spectra (rotatory strength vs wavelength) for the low- energy structures given in Figure 3 (A, (*R*)-1-NpOH (*na*) geometry; B, (*R*)-1-NpOH (*et*) geometry; C, (*S*)-1-NpOH (*na*) geometry; D, (*S*)-1-NpOH (*et*) geometry).

was more deeply included in the CD cavity for the *S*-enantiomer when compared to (*R*)-1-NpOH (Figure 3). In the case of the (*et*) geometry for (*S*)-1-NpOH, the ethyl group was not included as deeply in the CD cavity and the naphthyl axis was less tilted when compared to the structure calculated for (*R*)-1-NpOH (Figure 3). Positions of the guest facing the CD rim with the primary alcohols were also considered within the DMC runs, but in all complexes, involving either 1-NpOH or 2-NpOH, the energies of these structures were substantially higher than those observed for interaction with the rim containing the secondary alcohols.

ICD spectra were calculated for the structures with low energies. The two high-energy bands (short wavelengths) for the ICD spectra of (*R*)-1-NpOH complexed to β-CD were calculated to be strong and to have positive signals for the (*na*) and (*et*) geometries (Figure 4). A weak band around 270 nm was negative for most of the (*na*) structures with the low energies used, but this band was always positive for the complexes with the (*et*) geometries. In the case of (*S*)-1-NpOH, the ICD spectra calculated showed that for the (*na*) geometry the signals at high energy were positive, whereas a weak signal around 270 nm with negative sign was observed. In contrast the (*et*) geometry for (*S*)-1-NpOH showed a reversal of the signs for the bands at 270 and 205−210 nm (Figure 4).

The energies calculated for the (*na*) and (*et*) geometries

**Table 1. Potential ($E_P$, $\Delta E_P$), Solvation ($E_S$, $\Delta E_S$), and Total Energies ($E_C$) in kilocalories per mole for the 1:1 Complexes between (*R*)- and (*S*)-1-NpOH and *β*-CD Considering the *na* and *et* Configurations**

| configuration | $E_P$ | $\Delta E_P$ | $E_S$ | $\Delta E_S$ | $E_C$ |
|---|---|---|---|---|---|
| *R* (*na*) | 59.2 | −18.8 | −41.9 | +7.2 | −11.7 |
| *R* (*et*) | 56.9 | −21.2 | −44.1 | + 4.9 | −16.3 |
| *S* (*na*) | 55.8 | −23.6 | −49.9 | −0.9 | −24.5 |
| *S* (*et*) | 59.7 | −19.7 | −42.8 | + 6.2 | −13.5 |

of the complexes between (*R*)- and (*S*)-1-NpOH with *β*-CD yielded similar energies, with the (*et*) geometry being favored for the *R*-enantiomer and the (*na*) geometry having a lower energy for (*S*)-1-NpOH. Validation of the calculated structures can be obtained by comparing the calculated ICD spectra with the experimentally determined ones, because the ICD spectra are very sensitive to the position of the chromophore within the CD framework. This method is used to discriminate between different structures of similar energies. The important features to compare for the calculated and experimental ICD spectra are the progression of the bands and their sign, because some systematic deviations can be observed for the absolute energy values (wavelengths) of the calculated bands. The calculated spectra for the complexes between 1-NpOH and *β*-CD showed signals that in the experimental spectra appear around 270−290 nm and below 240 nm. The features between 240 and 250 nm do not appear in the calculations, because they are probably of vibronic nature. The difference in the calculated spectra for the (*na*) and (*et*) geometries of the (*R*)-1-NpOH/*β*-CD complex was the sign of the signal at 270 nm that was negative in the case of the (*na*) geometry and positive for the (*et*) geometry. The experimental ICD spectra showed a negative band in this spectral region, suggesting that the (*na*) geometry was present in solution. However, this assignment contradicts the structural calculations where the (*et*) geometry was shown to have the lowest energy and the triplet−triplet absorption spectra that suggest that the naphthyl ring was fairly exposed to the aqueous phase. A similar contradiction was observed for the (*S*)-1-NpOH/*β*-CD complex. In this case, the calculated ICD spectra showed that the bands at 270 and below 200 nm were respectively negative and positive for the (*na*) geometry, whereas the opposite signs were calculated for the (*et*) geometry. The experimental ICD spectrum has a negative band in the low-energy region (long wavelengths), suggesting the presence of a structure with the (*na*) geometry, whereas the strong negative band observed at 205 nm suggest the presence of the structure with the (*et*) geometry. The negative signal at high energy was very prominent and strongly suggests the presence of the (*et*) geometry for the (*S*)-1-NpOH/*β*-CD complex, although this structure was calculated to be of higher energy than the (*na*) geometry.

The poor correlation between the calculated ICD spectra and the experimental spectra strongly suggests that the (*na*) and (*et*) geometries were formed for both enantiomers of 1-NpOH. Interconversion between the two geometries is likely to occur after exit of the guest from the CD cavity into the aqueous phase, since the dynamics of exit and entry occurs on the microsecond time scale. In this respect, the complexation dynamics is fast and the ICD spectrum records a snapshot of complexes with both geometries. Stereoselectivity for the complex formation between 1-NpOH and *β*-CD would have been expressed if we had observed that one geometry would have been preferentially formed for one of the enantiomers. The poor selectivity observed is probably due to the fact that the chiral moiety of 1-NpOH was not located in a rigid enough environment close to the chiral framework of the CD. In the case of the (*et*) geometries the ethanol moiety is located within the cavity, whereas for the (*na*) geometries the ethanol moiety is pointing away from the alcohol rim of the CD.

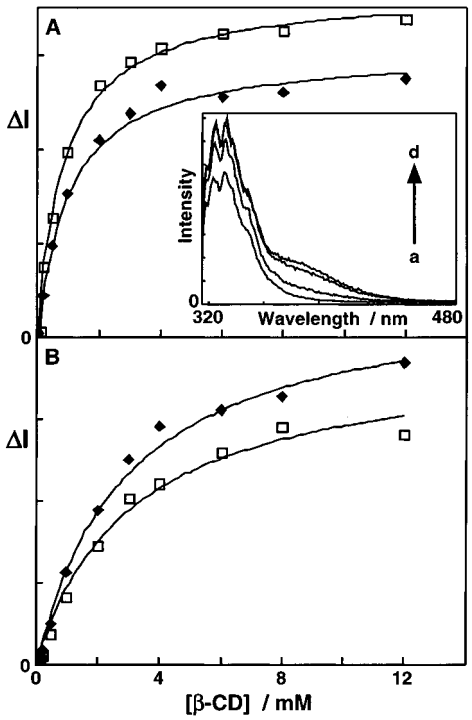


**Figure 5.** Fluorescence intensity changes for 150 *μ*M (*S*)-2-NpOH (□) and 150 *μ*M (*R*)-2-NpOH (◆) in the presence of various *β*-CD concentrations at 324 nm for the monomer emission (A) and 405 nm for the excimer emission (B). The solid lines were added to show the trends in the intensity change. The inset shows the fluorescence spectra for 300 *μ*M (*R*)-2-NpOH in the presence of (a) 0, (b) 1, (c) 5, and (d) 10 mM *β*-CD.

**Complexation of 2−NpOH with *β*-CD.** (*R*)- and (*S*)-2-NpOH form 1:1 ($K = 800$ M$^{-1}$) and 2:2 ($K = 3000$ M$^{-1}$) complexes with *β*-CD, but no stereoselectivity was observed within experimental errors for the equilibrium constant values of the 1:1 and 2:2 complexes.[36] The formation of the 2:2 complex led to excimer emission from 2-NpOH. Laser flash photolysis and $^1$H NMR experiments determined that the dissociation of the 2:2 complex was significantly slower (ca. $10^3$ s$^{-1}$) than the dissociation of 2-NpOH from *β*-CD in a 1:1 complex ($1.8 \times 10^5$ s$^{-1}$).[36]

The changes in the monomer and excimer intensities were reinvestigated at higher 2-NpOH concentrations. Increases in the monomer and excimer intensities were observed with increasing concentrations of *β*-CD (inset Figure 5). The fraction of 2-NpOH in the 2:2 complex increases when the 2-NpOH concentration was increased at a constant CD concentration. A stereoselectivity was observed for the magnitude of the monomer and excimer intensities. The monomer emission intensity at high *β*-CD concentrations was smaller for the *R*- than for the *S*-enantiomer (Figure 5). The opposite trend was observed for the change in the excimer emission, where the intensity for (*R*)-2-NpOH was higher than for (*S*)-2-NpOH. These trends were the same at 150 and 300 *μ*M 2-NpOH.

The excitation spectra recorded for the emission at 360 (mainly monomer) and 405 nm (mainly excimer) showed a broadening of the weak band around 320 nm for the excimer emission. In contrast, no shifts in this spectral region were apparent in the absorption spectra of both enantiomers in the presence of *β*-CD. In addition, in the time-resolved experiments no fast decay or growth was observed respectively for the monomer and excimer

emissions. These experiments suggest that excimers were formed within the time resolution of our single photon counter (<2 ns). The decays for the excimer emission of (*R*)- and (*S*)-2-NpOH (300 μM) in the presence of 10 mM β-CD were adequately fitted to the sum of two exponentials. The recovered lifetimes were the same for both enantiomers and corresponded to 34 ± 2 and 70 ± 2 ns. When the fluorescence for the same samples was collected for the monomer emission, a monoexponential decay with a lifetime of 38 ns was recovered. This value is the same as that determined previously.[36] The shorter lifetime observed for the excimer emission corresponds to the underlying emission of the monomer in this spectral region, whereas the longer lifetime corresponds to the excimer decay. The fact that the excimer lifetimes are the same for the *R*- and *S*-enantiomers shows that the difference in the steady-state intensity observed is not due to formation of different types of excimers with different lifetimes.

The triplet−triplet absorption maximum of 2-NpOH shifted from 413 nm in water to 416 nm when β-CD (10 mM) was added to the solution (Figure 1). The fwhm narrowed from 19 to 12 nm for 150 μM of 2-NpOH and 9−10 nm for 50 μM of 2-NpOH (inset Figure 1). For the former condition the fractions of 2-NpOH free in the aqueous solution and complexed as 1:1 and 2:2 complexes were respectively 0.08, 0.60, and 0.32. For 50 μM 2-NpOH in the presence of 10 mM β-CD, the fractions for free 2-NpOH and bound in 1:1 and 2:2 complexes were respectively 0.09, 0.74, and 0.17. Therefore, the triplet−triplet absorption signals were primarily due to complexed NpOHs, but the fractions of CD bound 2-NpOH with a 2:2 stoichiometry were 35 and 19% at the higher and lower guest concentrations, respectively. The triplet−triplet absorption spectra for 2-NpOH in the presence of β-CD show a larger red shift than was observed for 1-NpOH, and a decrease of the fwhm was also apparent. These results suggest that the naphthyl chromophore was more protected from the aqueous environment for both enantiomers of 2-NpOH. The narrowing of the bandwidth was more pronounced at the low 2-NpOH concentration (50 μM), where 80% of the guest formed a 1:1 complex. As the contribution of the 2:2 complex increased, the narrowing of the band was less pronounced, suggesting that for the 1:1 complex the naphthyl moiety was located in a more defined and rigid environment.

The ICD spectra for both enantiomers of 2-NpOH were measured at different 2-NpOH to β-CD concentration ratios in order to vary the relative amounts of the 2:2 and 1:1 complexes. For 50 μM 2-NpOH and 10 mM β-CD, the fractions of free and bound 2-NpOH are given above and the percentage of bound 2-NpOH that was in the form of a 2:2 complexes was low (19%). For 300 μM 2-NpOH and 1 mM β-CD the fractions of 2-NpOH free in solution and bound as 1:1 and 2:2 complexes were respectively 0.43, 0.35, and 0.22 and the percentage of bound 2-NpOH in the form of the 2:2 complex was higher (39%). (*R*)- and (*S*)-2-NpOH showed circular dichroism signals in water below 240 nm that are mirror images of each other. In the presence of β-CD, the ICD spectra correspond mostly to signals due to the inclusion of 2-NpOH into the CD cavity. At 50 μM 2-NpOH/10 mM β-CD (Figure 6) the differences observed for the ICD spectra of the *R*- and *S*-enantiomers were in the 240 and 200 nm regions. The fraction of free 2-NpOH for these conditions was small, and no changes were observed for the spectrum when a correction for signals due to the free 2-NpOH was performed.

At the higher 2-NpOH concentration ([2-NpOH] = 300 μM and [β-CD] = 1 mM) the percentage of free 2-NpOH

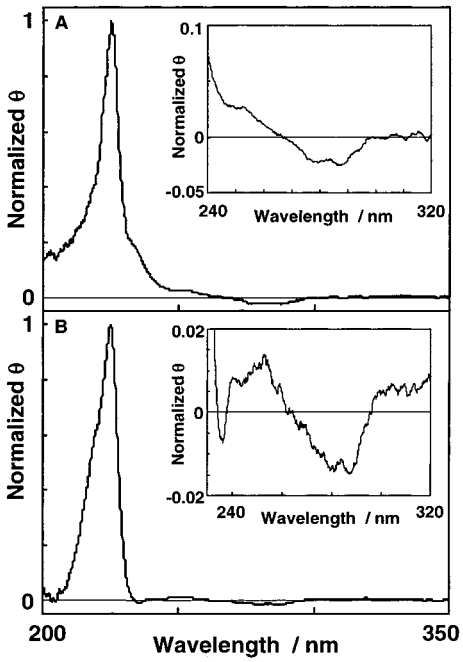


**Figure 6.** Combined and normalized ICD spectra for 50 μM (*R*)-2-NpOH (A) and 50 μM (*S*)-2-NpOH (B) in the presence of 10 mM β-CD. The normalization to unity corresponds to 4.1 and 4.8 mdeg ($l$ = 1 mm) in A and B, respectively. The insets are expansions of the ICD spectra.

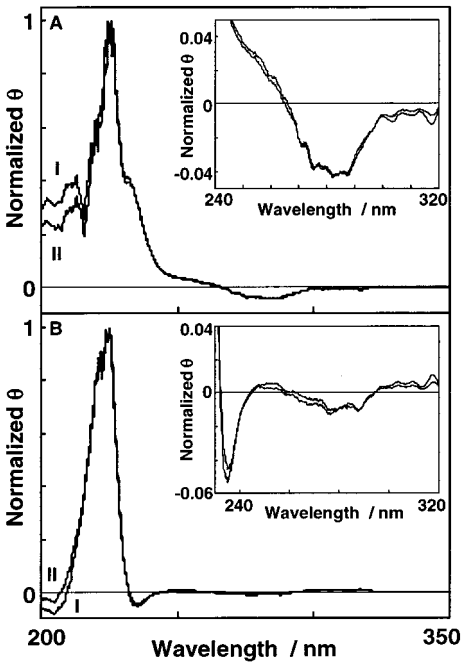


**Figure 7.** Combined and normalized ICD spectra for 300 μM (*R*)-2-NpOH (A) and 300 μM (*S*)-2-NpOH (B) in the presence of 1 mM β-CD (I). Spectra labeled as II are corrected for the ICD signals of the 2-NpOH fraction free in the aqueous phase. The normalization to unity corresponds to 9.1 (I), 8.9 (II) mdeg and 14.5 (I), 14.3 (II) mdeg ($l$ = 1 mm) in A and B, respectively. The insets are expansions of the ICD spectra.

was significant, but the contribution of the free 2-NpOH to the circular dichroism signal was small (Figure 7). Besides intensity changes below 215 nm the spectral features for the uncorrected and corrected spectra were the same. The features that were enhanced when compared to the spectra at lower 2-NpOH concentrations were the ICD signals at 230−240 nm (positive for (*R*)-2-NpOH

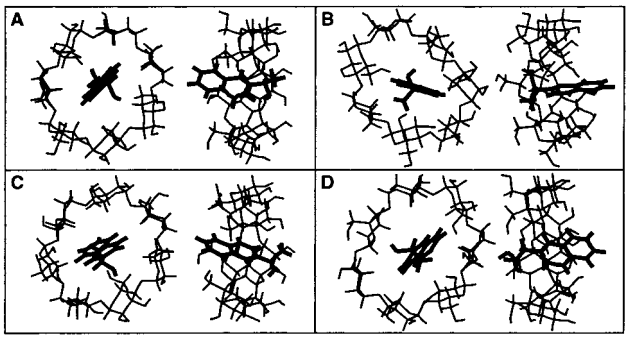


**Figure 8.** Low-energy structures calculated for the complexes with 1:1 stoichiometry between $\beta$-CD and (*R*)-2-NpOH (A, (*na*) geometry; B, (*et*) geometry) or (*S*)-2-NpOH (C, (*na*) geometry; D, (*et*) geometry).

**Table 2. Potential ($E_P$, $\Delta E_P$), Solvation ($E_S$, $\Delta E_S$), and Total Energies ($E_C$) in kilocalories per mole for the 1:1 and 2:2 Complexes between (*R*)- and (*S*)-2-NpOH and $\beta$-CD Considering the *na* and *et* Configurations**

| configuration | $E_P$ | $\Delta E_P$ | $E_S$ | $\Delta E_S$ | $E_C$ |
|---|---|---|---|---|---|
| 1:1 *R* (*na*) | 43.2 | −32.7 | −47.4 | + 2.0 | −30.7 |
| 1:1 *R* (*et*) | 52.7 | −23.2 | −44.7 | + 4.7 | −18.5 |
| 1:1 *S* (*na*) | 42.6 | −34.3 | −48.0 | +1.3 | −33.0 |
| 1:1 *S* (*et*) | 52.4 | −24.5 | −42.7 | + 6.6 | −17.9 |
| 2:2 *R* (*na*−*na*) | 58.9 | −92.9 | −46.6 | + 52.2 | −40.7 |
| 2:2 *R* (*na*−*et*) | 54.6 | −97.2 | −36.5 | +62.3 | −34.9 |
| 2:2 *R* (*et*−*et*) | 57.3 | −94.5 | −38.1 | +60.7 | −33.8 |
| 2:2 *S* (*na*−*na*) | 64.1 | −89.6 | −50.7 | + 48.0 | −41.6 |
| 2:2 *S* (*na*−*et*) | 63.2 | −90.5 | −43.7 | +54.9 | −35.6 |
| 2:2 *S* (*et*−*et*) | 61.0 | −92.7 | −42.5 | +56.2 | −36.5 |

and negative for (*S*)-2-NpOH) and the signals at 205−210 nm (positive for (*R*)-2-NpOH and negative for (*S*)-2-NpOH).

Complex formation between 2-NpOH and $\beta$-CD was in all cases driven by the changes in potential energies (Table 2). The structures for the 1:1 complexes for both enantiomers of 2-NpOH with the (*na*) geometry showed lower energies (ca. 15 kcal/mol) than the respective structures with the (*et*) geometry (Table 2). Indeed, the total energy values for the (*et*) geometries of the complexes with 2-NpOH were similar to those recovered for 1-NpOH complexes. The lower calculated energies for the (*na*) geometries correlate well with the higher binding affinity for the 1:1 complexes of 2-NpOH (800 $M^{-1}$) when compared to the affinity of 1-NpOH (160 $M^{-1}$). Stabilization of the (*na*) geometry was due to more favorable potential and solvation energies when compared to the (*et*) geometry. The structure with (*na*) geometry for 2-NpOH and $\beta$-CD showed a deeper inclusion of the naphthalene into the CD cavity (Figure 8) when compared to the 1-NpOH/$\beta$-CD complex. This deeper inclusion of 2-NpOH in the CD cavity can account for the narrowing observed for the triplet−triplet absorption spectra. In the case of the (*et*) geometries, the inclusion of 2-NpOH was shallower than for the (*na*) geometry and the CD ring was considerably distorted (Figure 8).

The calculated ICD spectra for the structures with lowest energies presented in Figure 8 show similar features (Figure 9). All spectra show large positive bands at high energies, as well as a small negative band around 270 nm. This negative band was always reproduced by low-energy structures corresponding to the (*na*) geometry of both enantiomers, but it was less frequently found for low-energy structures with the (*et*) geometry. Unfortunately the similar features obtained for the calculated ICD spectra for the (*na*) and (*et*) geometries makes it impossible to establish that only the (*na*) geometries were formed as suggested from the structural calculations. The

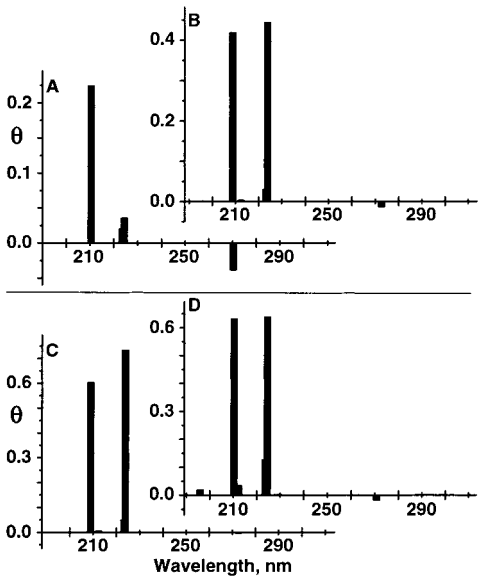


**Figure 9.** Calculated ICD spectra for the low-energy structures given in Figure 8 (A, (*R*)-2-NpOH (*na*) geometry; B, (*R*)-2-NpOH (*et*) geometry; C, (*S*)-2-NpOH (*na*) geometry; D, (*S*)-2-NpOH (*et*) geometry).

experimental ICD spectra for conditions where 80% of the complexed 2-NpOH was in the form of a 1:1 complex were different for the *S*- and *R*-enantiomers (Figure 6). This result contradicts the calculated ICD spectra. However, the differences observed can be explained by the contribution of the signals from the 2:2 complex since these differences were enhanced when the contribution of this latter complex was increased (Figure 7).

In the calculations involving higher order CD complexes the relative orientation of the host molecules has to be initially defined. Systematic studies on the interaction between the secondary and primary hydroxyl rims within CD-CD assemblies revealed that the most stable CD aggregates are formed when the secondary hydroxyl groups interact.[29] In this configuration the maximum number of intermolecular hydrogen bonds between the two CD molecules is formed. Therefore, this orientation was considered when calculating the higher order complexes between both enantiomers of 2-NpOH and $\beta$-CD. The 2:2 complexes can have three different geometries for the arrangement of the naphthyl moiety with respect to the CD secondary hydroxyl rim, i.e., (*na*−*na*), (*et*−*et*), and (*na*−*et*). The structures and energies of the 2:2 complexes were calculated for all three geometries (Table 2). The energies for the 2:2 complexes with (*na*−*et*) and (*et*−*et*) geometries were higher than for the (*na*−*na*) geometry, but the energy differences were smaller than observed between the (*na*) and (*et*) 1:1 complexes for (*R*)- and (*S*)-2-NpOH. It is also worth noting that the energetic differences between the 2:2 complexes with different geometries were mainly due to differences in the changes of the solvation energies. Tight 2:2 complexes were formed for both enantiomers (Figure 10). In the case of the (*na*−*na*) geometry for the *R*-enantiomer, a perfect alignment of the two host molecules was achieved that resulted in strong intermolecular hydrogen bonding between the two CDs, whereas in the case of the (*na*−*na*) geometry for (*S*)-2-NpOH the alignment of the two CD was somewhat offset. The low-energy structure of the (*na*−*et*) placed one naphthyl group deep in the CD cavity, whereas the second one was at the interface between the two CD molecules. In the (*et*−*et*) geometry the two naphthyl moieties were located at the interface formed by the interaction of the

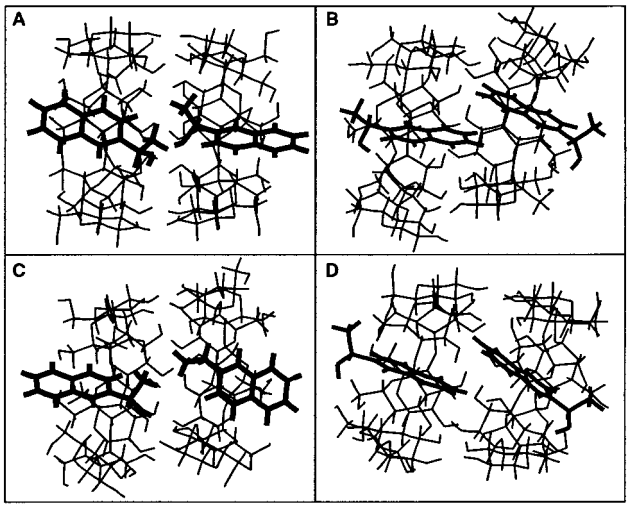


**Figure 10.** Low-energy structures calculated for complexes with 2:2 stoichiometries between ***β***-CD and (*R*)-2-NpOH (A, (*na*−*na*) geometry; B, (*et*−*et*) geometry) and (*S*)-2-NpOH (C, (*na*−*na*) geometry; D, (*et*−*et*) geometry).

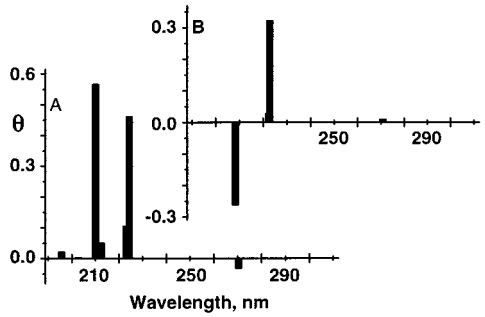


**Figure 11.** Calculated ICD spectra for the low-energy structures of the 2:2 complexes with the (*na*−*na*) geometries given in Figure 10 (A, (*R*)-2-NpOH; B, (*S*)-2-NpOH).

rims of the CD containing the secondary alcohols (Figure 10). In contrast to the (*na*−*na*) geometry, the two CD molecules were somewhat offset for the *R*-enantiomer, whereas the alignment was better for (*S*)-2-NpOH.

The calculated ICD spectra for the low-energy 2:2 complexes with (*na*−*et*) and (*et*−*et*) geometries show a series of bands with positive signs for both enantiomers. Therefore, these geometries cannot be discriminated from ICD measurements. The ICD calculations for the (*na*−*na*) geometries showed distinct differences for both enantiomers (Figure 11). In the case of (*R*)-2-NpOH, a negative signal was observed at 270 nm followed by three positive bands at lower wavelengths. In addition, the band below 200 nm had a smaller rotatory strength than the bands between 210 and 225 nm. For the *S*-enantiomer the band at 270 nm was positive, whereas at higher energies a negative band was observed. The magnitude for this latter band varies among different low-energy structures with the (*na*−*na*) geometry, but its sign was always negative for (*S*)-2-NpOH.

The 2:2 complex between 2-NpOH and β-CD could in principle have the (*na*−*na*), (*na*−*et*), or (*et*−*et*) geometries. On the basis of the fact that the (*na*) geometry for the 1:1 complex was calculated to have lower energies than the (*et*) geometries, we expected to see a clear preference for the (*na*−*na*) geometry in the case of the 2:2 complexes. However, the energy differences calculated between the geometries for the 2:2 complex are much smaller than those observed between the (*na*) and (*et*) geometries for the 1:1 complexes. It is also interesting that the differences arise mainly due to differences in the solvation energies of the 2:2 complexes, whereas for the 1:1 complexes significant changes were observed for both the changes in potential and solvation energies. This result seems to indicate that the enthalpic gains were similar for different molecules within the cavity of the two CDs, but the solvation of complexes with different geometries was significantly different. From the energetic point of view no stereoselectivity is apparent for the different 2:2 complexes. The (*na*−*na*) complexes were calculated to have the lower energies. Their presence is supported by the calculated ICD spectra. The inversion of the peaks at high and low energies for the two enantiomers was found consistent with the pattern shown by the experimental spectra. At 270 nm the calculated spectra predict a negative signal for the *R*-enantiomer and a positive one for (*S*)-2-NpOH. When the relative amount of the 2:2 complex was increased the magnitude of the negative band between 270 and 290 nm in the experimental ICD spectra decreased for the *S*-enantiomer when compared to the spectrum for (*R*)-2-NpOH (compare Figures 6 and 7). The second feature that differentiates the calculated ICD spectra for the (*na*−*na*) 2:2 complex was the sign of the band at high energies. This feature was also reproduced in the experimental spectra. The calculated ICD spectra for the other two geometries did not show any bands with negative signs, clearly indicating that the (*na*−*na*) geometry was present for the 2:2 complex of (*S*)-2-NpOH.

The formation of the 2:2 complex led to the observation of excimer emission and a long-lived triplet state. These two results cannot be reconciled by a geometry for the 2:2 complex where the naphthyl moieties are in close proximity so that excimer emission is observed. For such a geometry one would not expect to detect a long-lived triplet state since self-quenching is likely to be efficient. Indeed, excimer-like emission has been previously observed for the 2:2 complexes of α-terthiophene with γ-CD[46] and naphthalene with β-CD.[27] In both cases the authors did not observe a long-lived triplet and explained self-quenching as a likely reaction for the absence of this species. In the case of the 2:2 complex between naphthalene and β-CD, calculations similar to those performed in this work showed that the two guest molecules can move relatively freely within the 2:2 complex.[27] This degree of freedom explains the formation of the excimer and efficient self-quenching. In the (*na*−*na*) 2:2 complex with 2-NpOH, the ethanol moieties lock the naphthalenes into the CD cavity and the excited triplet state on one of the naphthalene moieties does not interact with the other naphthalene, leading to the detection of the long-lived triplet. Therefore, the formation of the (*na*−*na*) geometry explains the presence of the long-lived triplet. However, the (*na*-*na*) geometry cannot be responsible for the excimer emission because the formation of excimers occurs in less than 2 ns. If the 2-NpOH could move within the (*na*-*na*) geometry to form the excimer self-quenching would also occur. The excimer emission is likely to occur for the 2:2 complexes with the (*et*-*et*) geometry where the naphthalene moieties are located in close proximity. These results strongly suggest that in the case of the 2:2 complex a mixture of geometries is present. Finally, this mixture of geometries also explains the different monomer-to-excimer intensity ratios observed for the *R*- and *S*-enantiomers. This difference cannot be due to different equilibrium constants for the formation of the 2:2 complex since the same $K_{eq}$ values were observed,[36] neither can the difference

(46) De Feyter, S.; van Stam, J.; Imans, F.; Viaene, L.; De Schryver, F. C.; Evans, C. H. *Chem. Phys. Lett.* **1997**, *277*, 44.

be due to different types of excimers formed for each enantiomer because the lifetimes for the excimer emission were the same. Therefore, the lower excimer intensity observed for (*S*)-2-NpOH suggests that for this enantiomer a higher fraction of the 2:2 complexes has the (*na*−*na*) geometry.

## Conclusions

No stereoselectivity was observed for the 1:1 complexes of the enantiomers of 1-NpOH with $\beta$-CD. This situation arises because, from the topological point of view, the ethanol moiety from 1-NpOH is not sufficiently restricted by the CD framework. The point of importance in this system is that a mixture of complexes with different structures is formed for each enantiomer. Consequently, the measured complexation equilibrium constants and rate constants constitute a measurement for an ensemble of structures and not measurements for a precisely defined structure. In addition, this report clearly illustrates that structural calculations for ideally isolated molecules do not always provide a complete picture of the complexation behavior and validation of the calculations with directly predicted experimental observables is important. The formation of a mixture of complexes was revealed by the comparison of the calculated and experimental ICD spectra and was not immediately apparent from the structural calculations.

Stereoselectivity was observed for the 2:2 complexes of (*R*)- and (*S*)-2-NPOH with $\beta$-CD in the form of different monomer to excimer intensity ratios, but it was not apparent from the DMC calculations. The stereoselectivity is due to subtle structural changes of the 2:2 complexes that lead to mixture of geometries with different contributions of the (*na*−*na*) and (*et*−*et*) geometries. The formation of complexes with different geometries also explains why in the case of 2-NpOH excimer emission and a long-lived triplet were observed concomitantly. This result contrasts previous reports for naphthalene[27] where the guest is fairly free to move in the 2:2 complex, suggesting that anchoring in 2:2 complexes can be achieved by adding short spacers to the guest molecules.

In summary, we showed that the interaction of the enantiomers of 1- and 2-NpOH with $\beta$-CD is complex because mixtures of structures with different geometries are present. These studies also established that stereoselectivity in the rigid 2:2 complexes is more readily observed than in the more flexible 1:1 complexes.

**Acknowledgment.** C.B. thanks the Natural Science and Engineering Research Council of Canada (NSERC) and B.M. thanks the Austrian Academy of Sciences within APART (Austrian Program for Advanced Research and Technology) for the support of their research programs. R.S.M. thanks NSERC and the University of Victoria for graduate scholarships, whereas T.C.B. thanks the Conselho Nacional de Desenvolvimento Científico e Tecnológico, CNPq (Brazil) for a postdoctoral fellowship. The authors at the University of Victoria thank L. Netter for support in software development and Cerestar for their kind gift of the cyclodextrin samples.

LA0005311